To cite this article: HE W P, LIU M, WEI J H, et al. Analysis on compression behavior of woven carbon fiber reinforced thick composite laminates under low velocity impact[J/OL]. Chinese Journal of Ship Research, 2023, 18(5). http://www.ship-research.com/en/article/doi/10.19693/j.issn.1673-3185.03256 (in both Chinese and English).

DOI: 10.19693/j.issn.1673-3185. 03256

Analysis on compression behavior of woven carbon fiber reinforced thick composite laminates under low velocity impact

*HE Weiping[1], LIU Ming[1], WEI Jianhui[*1], KANG Fenghui[2], GE Xinxin[3,4], ZHANG Pan[*4]*

1 Wuhan Second Ship Design and Research Institute, Wuhan 430205, China

2 Luoyang Ship Material Research Institute, Luoyang 471023, China

3 China Ship Scientific Research Center, Wuxi 214082, China

4 School of Naval Architecture and Ocean Engineering, Huazhong University of Science and Technology, Wuhan 430074, China

Abstract: [**Objectives**] In order to study the effects of impact damage on the compressive strength and failure modes of woven carbon fiber reinforced thick composite laminates, in-plane compression tests are carried out. [**Methods**] The modified Hashin failure criterion and material degradation model are implemented with user-defined subroutines to simulate the failure behaviors of laminates using the ABAQUS/Explicit modelling package. The effectiveness of the numerical model is validated through comparison with experiments aimed at the compressive strength and failure modes. [**Results**] The results show that the impact damage reduces the compressive strength of the impacted laminates. The compressive failure mode of the non-destructive specimen is concentrated at the ends of the impacted laminates, while truncated failure occurs across the middle region. The compressive strength decreases with the increase of impact energy, but there is no linear relationship between the compressive strength and impact energy. The evolution of the damage behavior of laminated plates is closely related to the history of compression load. The damage failure of laminates hardly develops when the compression load is below the threshold of the failure load. Otherwise, the damage expands rapidly in the width direction, and compression damage eventually occurs across the whole width direction of the laminate. [**Conclusions**] The results of this study can provide references for evaluating the impact resistance of woven carbon fiber reinforced thick composite laminates.

Key words: carbon fiber reinforced composite; compression after impact; compressive strength; failure mode; finite element analysis (FEA)

CLC number: U661.4; TB332

0 Introduction

Carbon fiber composites have been widely applied in aerospace, automotive, ship, and medical fields due to their exceptional mechanical properties, fatigue and corrosion resistance[1]. In ship engineering, ship composites are often subject to low-velocity impacts of other objects such as falling tools, wave impacts, floater, marine organism, and ship collisions during manufacturing, using, and maintenance process. As a result of these low-velocity impacts, woven composites can experience damages such as matrix cracks, delamination, fiber breaks, and pits, which can significantly reduce the load-bearing capacity of the structure and pose a serious threat to the safety of the structure. The impact resistance of ship structures has long been a research hotspot for designers[2-3]. In fact, thick woven carbon fiber

Received: 2023 – 01 – 31 **Accepted:** 2023 – 04 – 13

Supported by: National Natural Science Foundation of China (52171307)

Authors: HE Weiping, male, born in 1985, master degree, senior engineer

WEI Jianhui, male, born in 1986, Ph.D., senior engineer

ZHANG Pan, male, born in 1986, Ph.D., associate professor, doctoral supervisor. Research interest: impact dynamics of ship structure and protection design. E-mail: panzhang@hust.edu.cn

***Corresponding author:** ZHANG Pan, WEI Jianhui

composite laminates will be adopted at some specialized areas of real ships, making it crucial to study the impact resistance of this type of structure.

The study on compression damage in composite materials after impact has been a hot issue for scholars in China and abroad. Fan et al. [4] analyzed the compression failure behavior and characteristics of two types of woven composite laminates, and found that the failure modes varied depending on the materials used. Using ABAQUS software, Jia et al. [5] investigated the impact of different damage depths after low-velocity impact on the residual compressive strength of composite laminates. They found that the deeper the damage, the weaker the load-bearing capacity of the laminate. Through experimental discussion, Zhu et al. [6] examined the relationship of impact energy and damage area, with residual compressive strength after impact. They concluded that the damage area after impact is the main determining factor for the compressive strength of laminates. Cui et al. [7] studied the influence of impact energy on residual strength of laminates based on finite element model and found composite laminates had the impact energy threshold that caused a sharp decrease in the residual strength of laminates. Ma et al. [8] conducted experiments on the compression characteristics of woven laminates after impact of different energies and analyzed the relationship of crater depth and damage area with residual strength and impact energy. Xu [9] developed a simulation model to study the entire process of composite laminates from low-velocity impact to post-impact compression damage, and verified the effectiveness of the model through comparison with test results. Through digital image correlation (DIC), Tuo et al. [10] revealed the damage evolution process of composite laminates under compressive loading after impact. They found that the post-impact compressive strength decreased with increasing impact energy and number of impacts. With combination of experimental and simulation methods, Yang et al. [11] investigated the influence of punch diameter and impact energy on the residual compressive strength of woven composite laminates after impact. They observed that the residual compressive strength of the laminates increased with a decrease in punch diameter. He et al. [12] examined the compression damage mode of composite laminates after impact combining experimental measurements and numerical simulations. They analyzed the impact of crater depth and impact energy on the residual strength of composite laminates after impact. Li et al. [13] determined the compression failure mode of carbon fiber composite laminates after impact through experimental investigations. They also established a numerical model for compression after impact. Evci[14] conducted low-velocity impact tests on laminates with thicknesses ranging from 2 to 8 mm. The study revealed that, in thinner laminates, fiber fracture damage on the bottom surface was primarily induced by bending stresses. Additionally, the perforation energy, absorbed energy, peak deformation, and contact time of the laminates decreased with an increase in thickness compared to thicker laminates. Caminero et al. [15] compared the post-impact compressive properties of laminates with three different thicknesses (2, 3, 4 mm). They found that, at the same impact energy, thicker laminates exhibited greater bending stiffness and higher postimpact compressive strength.

Currently, the majority of studies on the post-impact compressive strength of composite materials concentrate on thin or medium-thickness laminates. The studies on the post-impact compressive strength of thicker laminates are lacking. Yet, in practical engineering applications, the thickness of laminates employed in specialized areas of ships are often large The thickness of some structures may even exceed 12 mm. Hence, it is necessary to research on the post-impact compressive strength of thick composite laminates. This paper primarily focuses on the study of compression damage behavior in woven carbon fiber reinforced thick composite laminates after impact and analyzes the influence of impact damage on compression strength and failure modes. Simultaneously, a numerical simulation model for composite compression with initial low-velocity impact damage is established. The improved Hashin criterion and a material degradation model based on damage variables are utilized to predict the post-impact compression performance ot the structure. The aim is to provide a foundation for the design and application of woven carbon fiber reinforced thick composite laminate in practical engineering.

1 Test equipment and method

1.1 Preparation of materials and specimens

The woven carbon fiber reinforced thick composite laminate consists of carbon fiber (T300-3K) twill flat fabric with an areal density of 387 g/m^2. The matrix material used is vinyl resin (430LV). The laminates were fabricated using the vacuum-assisted resin infusion (VARI) molding process at a temperature of 23 ℃ and a pressure of approximately 0.1 MPa. Subsequently, specimens were cut into standard sizes of 150 mm×100 mm using a waterjet. Within the specimen, the carbon fiber content is approximately 68%, and the lay-up mode is $[(0,90)]_{60}$. The nominal thickness of a single layer is 0.22 mm.

1.2 Test device

For the study on the residual compressive strength of laminate after low-velocity impact, the tests primarily involve a low-velocity impact test and an in-plane compression test after impact. The low-velocity impact test was conducted using an Instron 9350 drop hammer impact tester in accordance with standard ASTM D7136. The punch was a steel hemisphere with a diameter of 16 mm and a mass of 5.5 kg, and the axis of the punch was perpendicular to the plane of the laminate. The experimental equipment has an anti-kickback system to prevent the laminate from repeated impacts. Fig. 1(a) shows the low-velocity impact test fixture.

After impact, compression experiment was performed on the specimens using a self-constructed compression tester in accordance with standard ASTM D7137. During the in-plane compression test on composite laminate, the laminate specimen was installed within the compression test fixture, making the specimen end flush with the end of the fixture. Pads located at the top and bottom of the fixture served to align and calibrate the specimen, as depicted in Fig. 1(b). Simultaneously, side plates with cutouts were positioned approximately 4 mm from the edge of the specimen. This could minimize out-of-plane bending caused by specimen buckling, preventing the overall instability of the restrained specimen. Sliding blocks support the bottom and top of the specimen to restrict any rotation of the specimen. The simply supported boundary conditions were assumed.

(a) Low velocity impact test fixture (b) Compression test fixture

Fig. 1 Low-velocity impact experiment fixture and compression test fixture

2 Numerical simulation model

2.1 Finite element model

Before the compression simulation experiment on composite laminate after impact, it is essential to initially predict the low-velocity impact test. After the low-velocity impact simulation experiment on the laminate, the low-velocity impact damage is introduced into the compressive finite element model using the restart analysis technique. Subsequently, axial compression was performed on the composite laminate containing impact damage, with a displacement load (U) applied, as illustrated in Fig. 2.

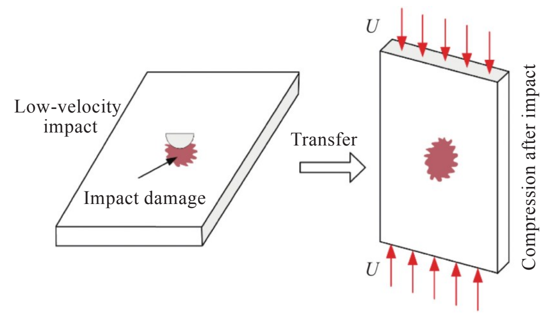

Fig. 2 Compression simulation analysis steps after impact

The ABAQUS 6.14/Explicit software was employed to create a three-dimensional finite element model of the woven carbon fiber reinforced thick composite laminate. The geometric dimensions of the laminate model are 150 mm×100 mm×13.2 mm, with a single layer thickness of 0.22 mm. The total number of layers is 60. 8-node linear solid unit (C3D8R) was chosen for the inner layer unit, while the interface unit (COH3D8) embedded in ABAQUS software was utilized to simulate interlayer layered damage. To capture the damage resulting from the low-velocity impact while ensuring computational efficiency and accuracy, local mesh refinement is implemented in the central impact region of the laminate. The in-plane size of the refined unit is set to 1 mm × 1 mm, covering a refinement range of 20 mm × 20 mm. Meanwhile, coarser meshes are applied in other regions. The compressed laminate model after impact should be consistent with the finite element model in low-velocity impact in terms of the number of units, material types, and material parameters. The differences only lie in the boundary conditions and loads. Simply support constraints are implemented at the bottom (left end) of the model to simulate the constraints on the specimen by the groove at the fixture's bottom. Displacement constraints in the thickness direction (U_3=0) are applied at the top and bottom sides of the model, simulating the constraints on the specimen by the cutter of the side plate of the fixture. A reference point (RP) is established on the right side of the model. Subsequently, through kinematic coupling constraints, all nodes on the top surface (right end) of the laminate are coupled to the reference point. Meanwhile, a velocity load (V) is applied to the reference point to simulate the compression test of the actual laminate. The model used in numerical simulation and the setting of boundary conditions are shown in Fig. 3.

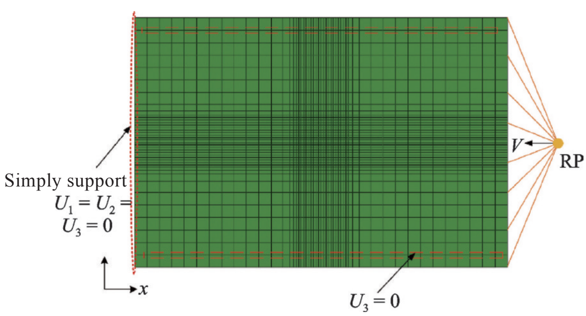

Fig. 3 FEM model and boundary conditions

2.2 Damage model

Woven composite laminates exhibit similar mechanical properties in both the longitude and latitude directions, making them anisotropic material in transverse and longitudinal directions. Throughout the damage process, the variation of strain components is smoother [16]. Hence, an improved Hashin failure criterion based on the strain form is employed to identify the initiation of unit damage, as illustrated below.

Longitudinal tensile failure ($\varepsilon_{11} \geqslant 0$):

$$f_{1\mathrm{t}} = \left(\frac{\varepsilon_{11} \cdot E_1}{X_\mathrm{t}}\right)^2 + \left(\frac{\varepsilon_{12} \cdot G_{12}}{S_{12}}\right)^2 + \left(\frac{\varepsilon_{13} \cdot G_{13}}{S_{13}}\right)^2 \tag{1}$$

Longitudinal compressive failure ($\varepsilon_{11} < 0$).

$$f_{1\mathrm{c}} = \left(\frac{\varepsilon_{11} \cdot E_1}{X_\mathrm{c}}\right)^2 \tag{2}$$

Transverse tensile failure ($\varepsilon_{22} \geqslant 0$):

$$f_{2\mathrm{t}} = \left(\frac{\varepsilon_{22} \cdot E_2}{Y_\mathrm{t}}\right)^2 + \left(\frac{\varepsilon_{12} \cdot G_{12}}{S_{12}}\right)^2 + \left(\frac{\varepsilon_{23} \cdot G_{23}}{S_{23}}\right)^2 \tag{3}$$

Transverse compression failure ($\varepsilon_{22} < 0$):

$$f_{2\mathrm{c}} = \left(\frac{\varepsilon_{22} \cdot E_2}{Y_\mathrm{c}}\right)^2 \tag{4}$$

Tensile failure in the thickness direction ($\varepsilon_{33} \geqslant 0$):

$$f_3 = \left(\frac{\varepsilon_{33} \cdot E_3}{Z_\mathrm{t}}\right)^2 + \left(\frac{\varepsilon_{13} \cdot G_{13}}{S_{13}}\right)^2 + \left(\frac{\varepsilon_{23} \cdot G_{23}}{S_{23}}\right)^2 \tag{5}$$

Compression failure in the thickness direction ($\varepsilon_{33} < 0$):

$$f_3 = \left(\frac{\varepsilon_{33} \cdot E_3}{Z_\mathrm{c}}\right)^2 \tag{6}$$

where f_i is utilized to identify the failure mode; ε_{ii} represents the strain component; E_i and G_{ij} denote the elasticity and shear moduli in the corresponding directions, respectively; X_t, X_c, Y_t, Y_c, Z_t, and Z_c are longitudinal tensile, longitudinal compressive, transverse tensile, and transverse compressive strengths, and tensile strengths and compressive strength in the thickness direction of a single-layer laminate, respectively; S_{ij} is the corresponding shear strength in the corresponding direction.

When $f_i \geqslant 1$, it indicates that the corresponding failure criterion is met, and the material model begins to suffer damage. Prior to the initial damage, the model exhibits a linear response, but once the initial damage occurs, there is a reduction in the model's stiffness. The continuous damage variable F_i (i = 1t, 1c, 2t, 2c, 3) is introduced to describe the initial and evolutionary processes of damage in the material and is calculated as follows:

$$F_i = \begin{cases} 0， & (f_i < 1;\ i = 1\mathrm{t}，1\mathrm{c}，2\mathrm{t}，2\mathrm{c}，3) \\ 1 - \dfrac{1}{f_i^n}， & (f_i \geqslant 1;\ i = 1\mathrm{t}，1\mathrm{c}，2\mathrm{t}，2\mathrm{c}，3) \end{cases} \tag{7}$$

where n ($n > 0$) is a dimensionless parameter to control the rate of damage evolution in woven composites. Taking into account the deterioration of material stiffness, the damage stiffness matrix $\boldsymbol{C}$ can be derived by inversion of the flexibility matrix $\boldsymbol{S}$.

$$\boldsymbol{C} = \boldsymbol{S}^{-1} = \begin{bmatrix} \dfrac{1}{E_1(1-w_1)} & -\dfrac{\upsilon_{12}}{E_2} & -\dfrac{\upsilon_{13}}{E_3} & 0 & 0 & 0 \\ -\dfrac{\upsilon_{12}}{E_2} & \dfrac{1}{E_2(1-w_2)} & -\dfrac{\upsilon_{23}}{E_2} & 0 & 0 & 0 \\ -\dfrac{\upsilon_{13}}{E_3} & -\dfrac{\upsilon_{23}}{E_2} & \dfrac{1}{E_3(1-w_3)} & 0 & 0 & 0 \\ 0 & 0 & 0 & \dfrac{1}{G_{12}(1-w_4)} & 0 & 0 \\ 0 & 0 & 0 & 0 & \dfrac{1}{G_{23}(1-w_5)} & 0 \\ 0 & 0 & 0 & 0 & 0 & \dfrac{1}{G_{13}(1-w_6)} \end{bmatrix}^{-1} \tag{8}$$

where υ_{12}, υ_{13}, and υ_{23} represent the Poisson's ratios corresponding to the 1-2, 1-3, and 2-3 planes, respectively; the stiffness reduction parameter w_i is determined by the damage variable F_i:

$$w_1 = \max(0, F_{1t}, F_{1c})$$

$$w_2 = \max(0, F_{2t}, F_{2c})$$

$$w_3 = \max(0, F_3)$$

$$w_4 = \max(0, F_{1t}, F_{1c}, F_{2t}, F_{2c})$$

$$w_5 = \max(0, F_{2c}, F_3)$$

$$w_6 = \max(0, F_{1t}, F_{1c}, F_3)$$

The Fortran language is utilized to encapsulate the material ontology, the enhanced Hashin failure criterion for the unit, and the stiffness degradation model of the damaged unit based on damage variables into a user-defined material subroutine. This subroutine is employed to conduct finite element simulations and analyze the compression process of composite laminates after low-velocity impact in ABAQUS/Explicit. Table 1 shows the primary material parameters for the woven carbon fiber reinforced thick composite laminate. In the table, t_n^0, t_s^0, and t_t^0 are the interfacial strengths in the normal direction, the 1st shear direction, and the 2nd shear direction, respectively; G_n^c and G_s^c are the release rates of fracture energy in the normal direction and the 1st shear direction, respectively; η is the mode coefficient.

Table 1 Mechanical properties of woven carbon fiber reinforced thick composite laminates [1]

Parameter	Numerical value
Density/(kg·m⁻³)	$\rho = 1\,467$
Elasticity parameter	$E_1 = E_2 = 62.3$ GPa, $E_2 = 8.5$ GPa $G_{12} = 7.1$ GPa, $G_{13} = G_{23} = 3.0$ GPa $\upsilon_{12} = \upsilon_{13} = \upsilon_{23} = 0.06$
Material strength/MPa	$X_t = Y_t = 610$, $X_c = Y_c = 314.7$ $Z_t = 55.6$, $Z_c = 500$ $S_{12} = 101.7$, $S_{13} = S_{23} = 59.4$
Interface parameters	$t_n^0 = 20$ MPa, $t_s^0 = t_t^0 = 34$ MPa $G_n^C = 0.32$ kJ/m², $G_s^C = 2.01$ kJ/m², $\eta = 2.09$

3 Analysis and discussion of results

3.1 Damage results

3.1.1 Low-velocity impact damage

The surface damage morphology of the woven carbon fiber reinforced thick composite laminate after a low-velocity impact was observed using an advanced digital microscope, and the results are depicted in Fig. 4. The results reveal that at an impact energy of 69 J, the laminate surface exhibits visible fiber breakage, splitting, and pit deformation. The splitting along the fiber direction results in the formation of cross-shaped cracks. With the increase of impact energy (99 J), the surface damage intensifies, and the features of pit deformation become more pronounced.

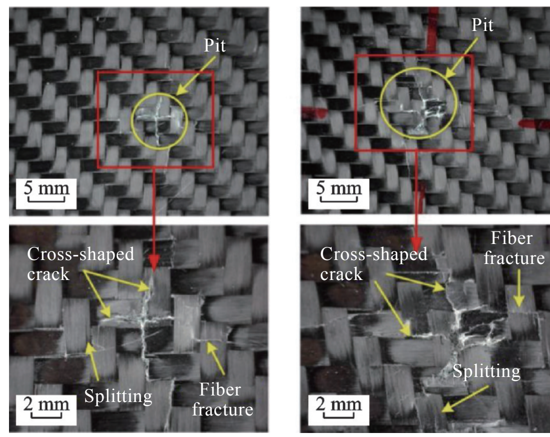

(a) 69 J impact energy (b) 99 J impact energy

Fig. 4 Impact damage on the surface of laminates

3.1.2 In-plane compression damage after impact

To quantitatively assess the influence of impact damage on the in-plane compression performance, in this study compression tests were conducted on woven carbon fiber reinforced thick composite laminates. The compression strength of the laminate in undamaged state and the residual compression strength after impact are listed in Table 2. The low impact-induced damage significantly will directly decrease the laminate's compressive strength; greater impact energy corresponds to increased damage and failure, resulting in a more pronounced reduction in compressive strength.

Table 2 Compression strength of laminates after impact

Impact energy/J	Number of specimens	Test compression strength/MPa	Simulated compression strength/MPa
0	1	314.4	303.0
69	2	219.1±1.3	256.4
99	2	208.5±2.5	208.6

The in-plane compression test for twill-woven carbon fiber reinforced thick composite laminate involved five working conditions (Table 2). For specimens impacted at room temperature, two repetitive tests were conducted at 69 J and 99 J impact energy. The relative errors of the test results were all within 2%, indicating good repeatability and reliability of the compression test results after impact.

Fig. 5 shows the compression failure modes of laminates after impact with different energies. It is apparent that in the absence of impact damage, compressive failure occurred at the end of the laminate. This is because that concentrated contact stresses are at the edge of the laminate and the loading indenter, resulting in end collapse and extensive longitudinal cracking. Under impact energies of 69 J and 99 J, truncated failure occurs across the middle region of the specimen, which can be explained by Saint-Venant principle. The initial impact damage defect significantly alters local stresses in the specimen during compression. However, its impact on stresses farther away from the defect is negligible. This ultimately leads to crack expansion and the formation of a penetrating fracture in the middle impact damage region.

(a) No impact energy

(b) 69 J impact energy

(c) 99 J impact energy

Fig. 5 Compression failure modes of laminates after impact with different energies

3.2 Finite element simulation results

3.2.1 Validation of numerical model

The numerical simulation results of the influence of low-velocity impact damage on the residual compressive strength of twill-woven carbon fiber reinforced thick composite laminates were compared with the experimental findings. The effectiveness of the numerical model was verified in terms of compressive strength and compression failure modes after impact. The compressive strength values obtained from tests and numerical simulations are compared, as shown in Table 2 The errors between numerical results and average test values are −3.6%, −17%, and 0% for impact energies of 0, 69, and 99 J, respectively. Given the material properties and external conditions, it is found that the compressive strengths derived from numerical simulations are in good consistence with the experimental results.

Compression failure of fiber is the predominant failure mode in woven carbon fiber reinforced thick composite laminate under compressive loading. The simulated compressive failure results from the numerical model are compared with the observed test results, and the results are shown in Fig. 6. For the laminate in the undamaged state, the numerically predicted failure mode is manifested as significant transverse fiber compression damage due to stress concentration at the end of the specimen, which agrees with the test results in Fig. 6(a). The failure modes of the laminates simulated numerically after both 69 and 99 J energy impacts were compressive failures across the entire middle of the composite laminate. In the post-impact compression tests, compressive failure occurred in the middle of the post-impact laminate along the entire width direction (Fig. 6(b) and Fig. 6(c)), and the results show that the numerical simulation results are in good agreement with the test results. In the simulation results, the nearly circular damage in the middle of the post-impact laminate model is the initial low-velocity impact damage, and the damaged area becomes larger with the increase of impact energy, which is in good agreement with the actual situation. In summary, the predicted location and extent of

(a) No impact energy

(b) 69 J impact energy

(c) 99 J impact energy

Fig. 6 Compression failure mode of the laminates compression failure using finite elements are in good agreement with the results observed in the tests, affirming the practicality and feasibility of the model in simulating compression failure behaviors of laminates.

3.2.2 Analysis of compression failure process

Take the case of 99 J impact energy as an example, the compression failure process of woven carbon fiber reinforced thick composite laminates after impact is analyzed. Fig.7 illustrates the longitudinal compression damage process. The value on the color bar indicates the unit damage state, ranging from 0 (initial non-destructive state) to 1 (complete failure state). From the figure, it can be observed that in the initial stage of compression, the damage to the composite laminate is attributed to the low-velocity impact simulation-induced impact damage. As the compression load reaches 80% of the laminate's failure load, the compression damage barely extends outward, with only the elements in the central impact-damaged region experiencing compression failure. As the compression load increases to 91% of the failure load of the laminate, the compression damage slowly expands along the width direction of the laminate model. Further increasing the compression load to 98% of the laminate's failure load results in a rapid expansion of compression damage along the width direction. When the compression load reaches 100% of failure load of the laminate, damage occurs across the entire width direction of the model, leading to the complete failure of the composite laminate structure.

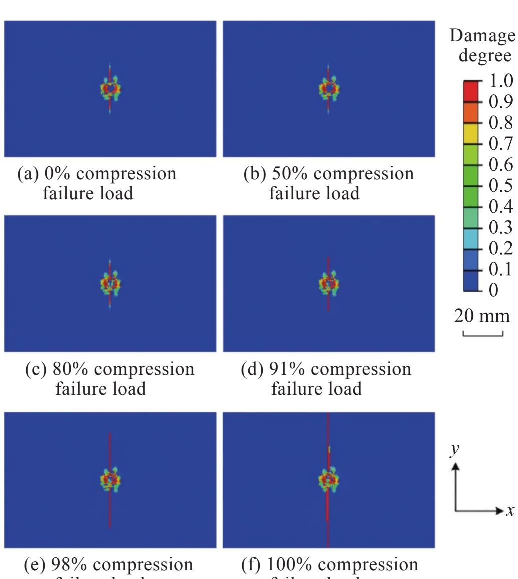

Fig. 7 Compression damage process of laminate after impact

4 Conclusion

In this paper, the compression tests after impact with typical energies were carried out for the compression behavior of twill-woven carbon fiber reinforced thick composite laminates after impact. Additionally, the numerical model was developed to predict the structural failure behavior of the laminates, and the effect of impact energy on compression behavior was investigated. The following conclusions are mainly obtained:

1) In the undamaged state, the compression damage mode of the woven carbon fiber reinforced thick composite laminate primarily is end compression damage. After impact, the thick laminate experiences truncated failure across the impact damage region. The presence of impact damage defects induces notable changes in local stress during compression, ultimately leading to crack expansion in the middle impact damage region. This contributes to the formation of a penetrating fracture, thereby reducing the compressive strength of the laminate.

2) The compressive strength after impact decreases with increasing impact energy, but there is no linear relationship between compressive strength and impact energy. With impact energies of 69 J and 99 J, the average compressive strength after impact decreases from 314.4 MPa to 219.1 MPa and 208.5 MPa, respectively, decreasing by 30.3% and 33.6%.

3) The development of user subroutines enables the simulation of compression damage behavior in twill-woven carbon fiber reinforced thick composite laminate. The validity and accuracy of the numerical model were confirmed through comparisons with experimental results.

4) During the compression process, the damage to the laminate does not significantly increase before the compression load reaches the threshold value for damage. Once this threshold is reached, the damage rapidly expands along the width direction. Eventually, the compression damage spreads across the entire width direction of the model.

References

[1] GE X X, ZHANG P, ZHAO F, et al. Experimental and numerical investigations on the dynamic response of woven carbon fiber reinforced thick composite laminates under low-velocity impact [J]. Composite Structures, 2022, 279: 114792.

[2] WU L, WANG Z H, LIU G C. Experimental analysis of damage response of glass fiber reinforced vinyl resin composite laminate under collision load [J]. Chinese Journal of Ship Research, 2019, 14 (Supp 1): 115 – 120, 134 (in Chinese).

[3] ZHU R X, BAI X F, MEI Z Y, et al. Experimental study on damage characteristics of hybrid carbon-glass fiber sandwich panel under low velocity impact [J]. Chinese Journal of Ship Research, 2020, 15 (4): 66−72 (in Chinese).

[4] FAN J J, ZHAO X, TAO C H, et al. Compressive failure of plain woven composite laminate with low velocity impact damage [J]. Polymer Materials Science and Engineering, 2010, 26 (5): 108−110 (in Chinese).

[5] JIA J D, DING Y L, HU B R. Numerical simulation of the compressive failure of composite laminates under low velocity impact [J]. Mechanical Science and Technology for Aerospace Engineering, 2010, 29 (10): 1320−1324 (in Chinese).

[6] ZHU W Y, XU X W. Experiment research on residual compressive strength and fatigue performance of composite laminates with low velocity impact damage [J]. Acta Materiae Compositae Sinica, 2012, 29 (5): 171−178(in Chinese).

[7] CUI H P, WEN W D, ZHANG A L. Influence of different impact energies on damage and residual strength of laminates [J]. Journal of Aerospace Power, 2015, 30 (10): 2331−2337 (in Chinese).

[8] MA S H, GUO H J, HUI L, et al. Low-velocity impact damage and compression failure behavior of plain woven composite laminate [J]. Journal of Aeronautical Materials, 2015, 35 (4): 39−44 (in Chinese).

[9] XU Y T, ZUO H F, LU X H, et al. Numerical analysis and tests for low-velocity impact damage evaluation of composite material [J]. Journal of Vibration and Shock, 2019, 38 (3): 149−155 (in Chinese).

[10] TUO H L, LU Z X, MA X P, et al. An experimental and numerical investigation on low-velocity impact damage and compression-after-impact behavior of composite laminates [J]. Composites Part B: Engineering, 2019, 167: 329 −341.

[11] YANG B, CHEN Y, LEE J, et al. In-plane compression response of woven CFRP composite after low-velocity impact: modelling and experiment [J]. Thin-Walled Structures, 2021, 158: 107186.

[12] HE Z L, LI X H. Residual strength analysis of impact damaged composite laminates [J]. Hi-Tech Fiber and Application, 2021, 46 (2): 15−20 (in Chinese).

[13] LI L, SONG G B, ZHENG H Y, et al. Numerical simulation and experimental validation of compressive residual strength of carbon fiber composite laminates with impact damage [J]. Chinese Quarterly of Mechanics, 2021, 42 (3): 498−506 (in Chinese).

[14] EVCI C. Thickness-dependent energy dissipation characteristics of laminated composites subjected to low velocity impact [J]. Composite Structures, 2015, 133: 508−521.

[15] CAMINERO M A, GARCÍA-MORENO I, RODRÍGUEZ G P. Experimental study of the influence of thickness and ply-stacking sequence on the compression after impact strength of carbon fibre reinforced epoxy laminates [J]. Polymer Testing, 2018, 66: 360−370.

[16] ZHANG G Q. Energy absorption and low velocity impact damage resistance of composite lattice structures [D]. Harbin: Harbin Institute of Technology, 2014 (in Chinese).

斜纹编织碳纤维复合材料层合厚板冲击后压缩行为分析

和卫平 [1], 刘明 [1], 魏建辉 [*1], 康逢辉 [2], 葛辛辛 [3,4], 张攀 [*4]

1 武汉第二船舶设计研究所, 湖北 武汉 430205

2 洛阳船舶材料研究所, 河南 洛阳 471023

3 中国船舶科学研究中心, 江苏 无锡 214082

4 华中科技大学 船舶与海洋工程学院, 湖北 武汉 430074

摘　要: [**目的**] 为分析冲击损伤对层合板压缩强度和失效行为的影响,对冲击后的编织碳纤维复合材料层合厚板开展面内压缩试验和数值仿真研究。[**方法**] 通过建立有限元模型,开展层合板冲击后的压缩仿真分析,采用 Fortran 语言编写用户自定义材料子程序(VUMAT),实现改进的 Hashin 失效准则和基于损伤变量的材料退化模型在 ABAQUS/Explict 中的应用;从压缩强度和压缩破坏模式两方面将数值模拟与试验结果进行对比,验证所建立数值模型的有效性。[**结果**] 结果显示,冲击损伤会降低层合板的压缩强度,无损层合板的压缩失效模式为端部破坏,冲击后的层合板会出现横贯试件中部的截断式破坏;冲击后的压缩强度会随冲击能量的增大而降低,但压缩强度与冲击能量之间并不存在线性关系;层合板损伤行为的拓展与压缩载荷的历程密切相关,压缩载荷在达到层合板破坏载荷的阈值之前,层合板的损伤几乎没有发生拓展,一旦压缩载荷达到阈值,损伤将沿宽度方向迅速拓展,最终发生横贯整个模型宽度方向的压缩损伤。[**结论**] 所做研究可为斜纹编织碳纤维复合材料层合厚板的抗冲击性能评估提供参考。

关键词: 碳纤维复合材料; 冲击后压缩; 压缩强度; 失效模式; 有限元分析